J. Fluid Mech. (1988), *vol.* 193, *pp.* 417–443
Printed in Great Britain

Reheat buzz: an acoustically coupled combustion instability. Part 1. Experiment

By P. J. LANGHORNE
Department of Physics, University of Otago, PO Box 56, Dunedin, New Zealand

(Received 21 August 1987)

Reheat buzz is a combustion instability which occurs in the afterburners of jet aeroengines. Similar oscillations have been observed on a laboratory rig in which a confined flame is stabilized in the wake of a conical gutter. The source of energy for the instability is the unsteady heat release as the flame responds to velocity fluctuations in the approach flow. The amount of energy fed into the instability is determined primarily by the phase relationship between the unsteady heat release rate and pressure fluctuations. Two types of relationship between pressure and heat release have been observed. In the first kind, perturbations in heat release rate convect downstream from the lip of the flame stabilizer at the axial velocity of the cold reactants. In the second type, which occurs downstream of the first, the phase of the heat release rate at the buzz frequency is constant and close to the phase of the unsteady pressure. The characteristics of the resulting instability depend on which of these occupies the larger portion of the duct. Consequently two types of instability exist and the transition between them occurs sharply, with little change in mean flow conditions. The transition is associated with an abrupt change in buzz amplitude and frequency as well as with a change in the shape of the modal distributions.

1. Introduction

The problem of combustion instabilities has existed for as long as man has attempted to use combustion to his advantage in confined systems. Such instabilities occur in units as diverse as residential oil-fired heaters to blast furnaces, rockets and jet aeroengines. The oscillations can be driven by pulsations in the supply of air or fuel, by fluctuations in mixture concentration, by periodic changes in fuel atomization (Putnam 1971; Putnam & Faulkner 1982) or by incomplete combustion (Schöyer 1983). In cases where there is a steady supply of fuel and air, resonance may still occur as a result of vortex shedding at the Strouhal frequency or as a consequence of the coupling between the unsteady heat release and pressure. Conventionally there are two possible solutions to the problem; either the damping in the system is increased, for example by including some type of acoustic liner, or the aerodynamics of the burner are modified so that the flame/sound field interaction is reduced (Baade 1978; Putnam 1971). In principal an indication of how these changes should be made can be found from a knowledge of the transfer function across the flame and the impedences on either side of it (Baade 1978; Mugridge 1980). In practice these quantities are rarely known with any accuracy.

Reheat buzz is a particular low frequency (50–150 Hz) combustion instability which occurs in the afterburners of jet aeroengines operating at high fuel to air ratios. Under these conditions, pressure fluctuations can become large enough to cause

severe structural damage (Lewis 1967). For the purposes of experimental modelling, the afterburner is generally replaced by a straight duct of uniform cross-section in which there is a significant mean flow of premixed gas. A similar instability also occurs here and we use the same term, reheat buzz, to describe it. Because the burning velocity of the flame is very much less than the mean gas velocity, the flame must be stabilized in a region of recirculation, such as the wake of a bluff body. Schlieren films (Jones, private communication) have shown that pressure waves incident on the gutter cause distortions of the flame front and hence local perturbations in heat release rate. The possibility of exciting longitudinal pressure waves then exists since Rayleigh's criterion (Rayleigh 1896) states that energy is fed into the instability if the unsteady heat release rate is in phase with the pressure fluctuations. Conversely, damping occurs if these quantities are out of phase. Energy is lost at the boundaries where it is radiated to the outside. Thus if conditions are such that the net gain of energy exceeds the losses, perturbations grow until nonlinear effects become important and the limit cycle is reached.

The fluid dynamic behaviour resulting in the unsteady combustion has previously been described as follows. Velocity fluctuations in the approach flow cause a burning vortex to be shed at the flame holder. This moves downstream with the local average speed of the reactants and products (Hedge *et al.* 1987), growing in size with axial position until it impinges upon the combustor wall. At this position mixing and combustion are intensified (Smith & Zukoski 1985) and the expansion of the gases generates a pressure wave and associated velocity fluctuation which triggers the next cycle. This interaction between forced vortex shedding and acoustics is also considered important by Sterling & Zukoski (1987) and Poinsot *et al.* (1987). The latter authors show the influence of the vortex shedding on the unsteady heat release rate. The frequency of this forced vortex shedding as well as the character and motion of the vortices is reported to depend on the magnitude of the instability (Keller *et al.* 1981). Conditions have been described which lead to a resonant frequency associated with a Strouhal number (Sivasegaram & Whitelaw 1987), to a resonant frequency determined by the overlap between an acoustic frequency and the frequency of a shear layer instability (Hedge *et al.* 1987) and to an acoustically-determined frequency (Heitor, Taylor & Whitelaw 1984). The acoustic nature of the instability is further demonstrated by the reported success of purely acoustic models with no provision for the addition of fluctuating energy to the flow (Clark & Humphrey 1986; Poinsot *et al.* 1987) or where combustion is treated as a volume source at the flame holder (Sterling & Zukoski 1987). While these models can predict the resonant frequencies of the geometries in question and match the measured pressure distribution with reasonable accuracy, they are unable to determine which modes are unstable. For identification of the dominant frequency of the instability, one must resort to measurement. Campbell, Bray & Moss (1983) describe a detailed investigation of an instability which does not appear to be acoustically coupled. Instead they identify the response time of the flame/flow interaction as the crucial parameter and show that the burning velocity is not a constant throughout a cycle. However, the large area ratio contraction at the upstream end of their apparatus made the acoustic boundary conditions difficult to evaluate. Such a geometry has subsequently been shown not to be susceptible to acoustically coupled combustion instabilities (Katsuki & Whitelaw 1986).

Comprehensive parametric studies of the factors influencing buzz have been carried out and we shall briefly summarize the most important conclusions. The onset of reheat buzz is crucially dependant on the local fuel to air ratio (Lewis 1967)

with the pressure amplitude increasing as the equivalence ratio, ϕ, (defined as the ratio of the mass of fuel to that of air as a fraction of the stoichiometric value) approaches unity. Likewise the buzz frequency peaks as ϕ approaches 1 from either the lean or rich regime (for example, Heitor *et al.* 1984). Increasing the approach velocity appears to increase the buzz frequency and reduce the amplitude where inconsistencies may well be due to concomitant changes in turbulence levels. The amplitude of the buzz oscillations is found to be maximum at intermediate values of gutter blockage ratio. If the stabilizer is moved downstream within a straight duct or there is an increase in the upstream length, the buzz frequency is reduced. In addition tests have been performed with different shapes of flame stabilizer (Heitor *et al.* 1984), with pilot flames as stabilizers (Katsuki & Whitelaw 1986) and with smooth and sudden contractions and expansions both upstream and downstream of the stabilizer (Vaneveld, Hom & Oppenheim 1984; Katsuki & Whitelaw 1986; Sivasegaram & Whitelaw 1987).

There is now a significant amount of experimental data concerning combustion instabilities in ducts with mean flow. This study differs in its emphasis on the concurrent development of theory and experiment and on the comparison of theoretical predictions with experimental results. For example, care has been taken to ensure the upstream boundary condition in the experimental set-up is compatible with theory and that it is a condition which isolates the acoustics of the working section from that of the supplies. This lack of knowledge of the boundary conditions is probably the most serious short-coming of many previous experiments. Our ultimate aim is to predict the frequency and onset fuel to air ratio for buzz in practical geometries. A model of the dynamic behaviour of the flame in response to an unsteady velocity field is therefore constructed and is used in calculations described in Bloxsidge, Dowling & Langhorne (1987) (hereinafter referred to as Part 2). The theoretical predictions are then tested against experimental data obtained on our rig in well-prescribed conditions. Extension of the model to more complex, but practically more interesting geometries is then possible (Bloxsidge 1987).

The apparatus used for the combustion experiments is described in §2. In §3 the radial uniformity of the mixing of fuel and air and the fluid dynamic conditions upstream of the flame holder are examined. The accuracy and reproducibility of the experiments is discussed, particularly for the unsteady measurements which are described in §4. The experimental results of §5 confirm previous observations of a coherent instability related to the acoustics of the configuration. New results, discussed in §6, show that there are two different types of coupling between the unsteady heat release rate and flow perturbations. In the one associated with small amplitudes of oscillation, perturbations in heat release rate convect along most of the duct at approximately the axial velocity of the reactants. In the other type, which occurs at higher fuel to air ratios, this behaviour extends only a short distance downstream of the gutter lip before the phase of the heat release rate at the buzz frequency assumes an almost constant value close to that of the unsteady pressure. The theory of Part 2 predicts the frequency, growth rate and mode shapes for either type of coupling.

2. Description of the apparatus

A blow-down apparatus is used for the combustion experiments with the advantage of providing a quiet air supply which is free from surges. The storage vessels hold sufficient air for the regulated supply pressure to be held constant for up

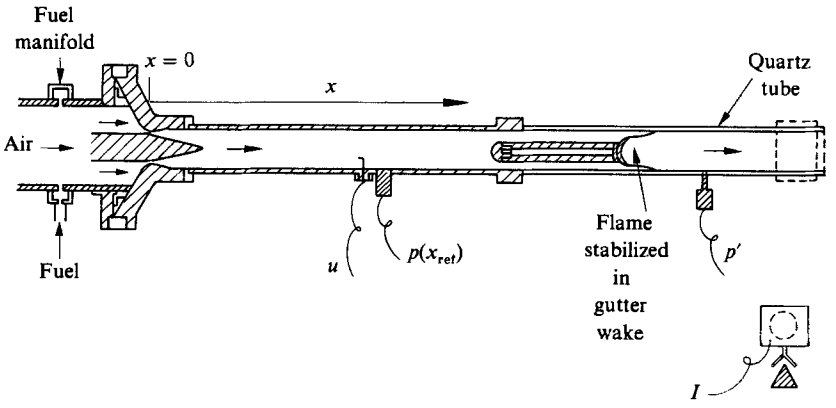

FIGURE 1. Sketch of experimental rig. Pressure (p), velocity (u) and C_2 emission intensity (I) are measured at axial positions (x) along the working section.

to 20 minutes at typical running conditions. The air pressure in the rig is operated pneumatically from a control room, the mass flow being metered by a venturi tube. Ethylene (C_2H_4) is injected into this flow through a manifold with ten 1.3 mm diameter holes around the circumference of the air duct (see figure 1). The flow of ethylene through these orifices is choked and the upstream pressure, and hence fuel flow rate, can be varied from the control room by means of a flexible drive to a pressure regulator. The regulator is mounted in a heated bath to prevent loss of regulator sensitivity due to excessive cooling on throttling the ethylene and to ensure the ethylene temperature remains constant during an experimental run. Without this precaution the fuel flow rate increases as the pipes cool.

Immediately downstream of the fuel manifold the fuel/air mixture is forced through a restriction and expands into the working section. The area of the restriction is chosen so that the flow of premixed gas is just choked at the desired running condition. This prevents acoustic disturbances from interfering with the air supply and provides a well-defined isentropic boundary condition at the upstream end of the working section. The working section is a cylindrical duct 70 mm in diameter. The flame stabilizes in the wake of a conical gutter mounted some distance downstream of the restriction. This length, and that from the gutter to the end of the duct, were varied in the experiments described in this paper. The duct upstream of the gutter support is stainless steel while the downstream length is quartz allowing optical access to regions just upstream as well as downstream of the gutter lip. The premixed gas is ignited 50 mm downstream of the gutter by pneumatically operated, retractable electrodes which sit flush with the wall of the duct in countersunk holes when burning has commenced. In order to avoid damaging pressure pulses, ignition takes place at a fuel flow rate well below design and air and fuel flow rates are then increased remotely to the desired running condition. The external walls of the quartz ducting are air-cooled and the laboratory is kept about 4 mbar above atmospheric pressure to encourage the discharge of combustion products through the exhaust ducting.

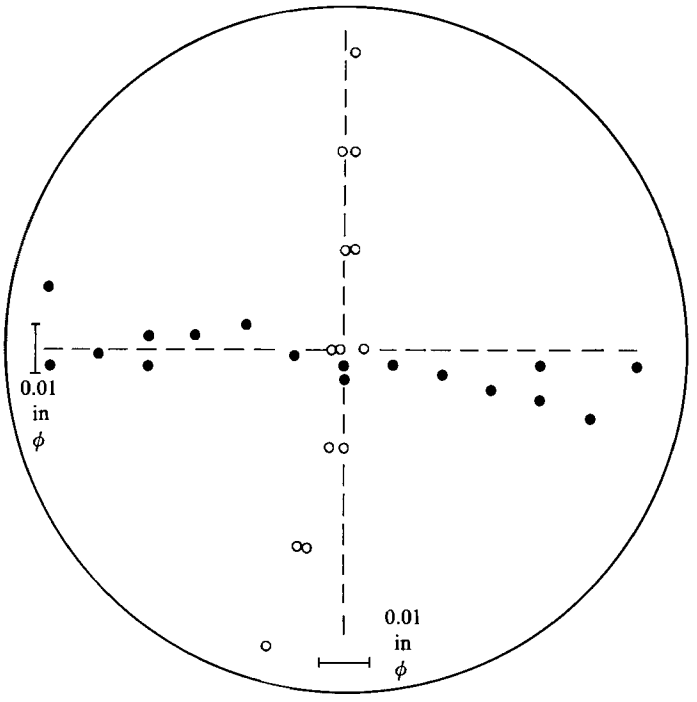

FIGURE 2. Profiles of local equivalence ratio across the duct diameter at $x = 0.70$ m, in the ●, horizontal and ○, vertical directions.

3. Mean flow conditions

The mass flow of premixed gas, Mach number and equivalence ratio upstream of the flame holder are logged and displayed on an LSI4 minicomputer with an absolute accuracy of $\pm 4\%$, $\pm 5\%$ and $\pm 5\%$ of typical values respectively. In addition short-term mean values of unsteady quantities are stored on minicomputer.

A simple gas-sampling apparatus is used to test the uniformity of mixing of fuel and air by measuring radial variations in equivalence ratio upstream of the flame holder. Two arms of a bridge, one of which is coated with a catalyst, are exposed to a flow of combustible mixture so that gas concentration is indicated by the differential heating of the arms. Four 0.2 mm diameter holes distributed at 90° around the circumference of a 3 mm diameter cylindrical probe extract the premixed gas sample. The sample is then mixed with dilution air and passed over the sensor some 15 diameters downstream. The sampling probe is mounted on a remote traverse gear which can be positioned with an accuracy of ± 1 mm. No attempt is made to obtain an absolute calibration of the probe since the sample flow rate is sensitive to static pressure in the rig. Instead the device was designed to measure radial variations and a datum is obtained each time it is used by equating the output of the sensor with the probe at the centre of the duct to the radially averaged value of ϕ deduced from air and fuel flow rates. Used in this way the repeatability of the gas sensor is approximately ± 0.005 in ϕ. Typical results at an approach Mach number of 0.08 at $x = 0.70$ m (figure 2) were found to give local variations in ϕ of 2% of the radially averaged ϕ in the horizontal direction and 3% in the vertical direction. We are satisfied that these variations are small enough for the assumptions of radial uniformity to be valid.

Velocity traverses performed at the same position show that the effects of the annular jet from the diffuser have been dissipated and will not influence the flame holding characteristics. The turbulent intensity in the flow upstream of the flame holder without combustion is of the order of 10% of the mean flow.

4. Instrumentation for unsteady measurements

All unsteady measurements are recorded on a RACAL STORE 7DS tape recorder with spectral analysis being performed on a Hewlett Packard Fourier Analyser. Measurements are decomposed into mean and fluctuating components so that pressure, for example, will be written as

$$p(x,t) = \bar{p}(x) + p'(x,t).$$

Examples of the power spectra of pressure and C_2 emission, to be described in sections 4.1 and 4.3 respectively, are shown in figure 3. These show the dominant nature of the buzz peak some 20 dB above the rest of the spectrum. The unsteady component at the buzz frequency can be expressed in the form

$$p'(x,t) = \mathrm{Re}\,[\hat{p}(x)\exp(\mathrm{i}\omega t)]$$

where $\hat{p}(x)$ is the complex amplitude at the buzz frequency, ω. High coherence was found at the buzz frequency between pressure and light signals for data from almost all parts of the duct enabling transfer functions to be accurately measured. Coherence levels indicate signal to noise ratios generally greater than 20 for regions where there are significant light fluctuations. The modulus and phase of transfer functions at the buzz frequency are plotted as a function of axial position along the duct. These are referred to a datum pressure measurement upstream of the combustion zone for both pressure, $\hat{p}(x)/\hat{p}(x_{\mathrm{ref}})$, and C_2 emission intensity per unit length, $\hat{\imath}(x)/\hat{p}(x_{\mathrm{ref}})$. The 95% confidence intervals for the true modulus and phase (Bendat & Piersol 1971) are also shown for all data points. The theoretical mode shape of the pressure upstream of the flame is deduced from the reflection of an acoustic wave at the measured frequency from the choked inlet restriction.

4.1. *Pressure*

Kistler Instrumentation 7031 piezoelectric transducers with charge amplifiers are used to make unsteady wall pressure measurements in the flame region. These are water-cooled and mounted on 0.7 mm diameter, 11 mm long stainless steel tubes which are sealed into the quartz duct. For frequencies of interest, the attenuation and phase shift due to the mounts are negligible in theory (Tidgeman 1975) and this was confirmed by experiment. In the region upstream of the flame a Gaelter 3EA/a transducer is flush-mounted to record mean and unsteady pressure. This transducer is calibrated before each set of experiments and measures fluctuations in pressure to better than $\pm 2\%$ of their amplitude. Since we are not only interested in the magnitudes of pressure, velocity and heat release but also in the relative phases between these quantities, it is important to know the phase shift introduced by any of the transducers or their associated electronics. Both types of transducer were therefore mounted at the same location along with a Brüel and Kjaer 4136 microphone and 2618 preamplifier for which the manufacturer supplied phase shift information. The microphone and its recording apparatus had previously been calibrated against a Brüel and Kjaer pistonphone at 103 Hz. In this way, the manufacturers calibration for the Kistler transducers was checked against the

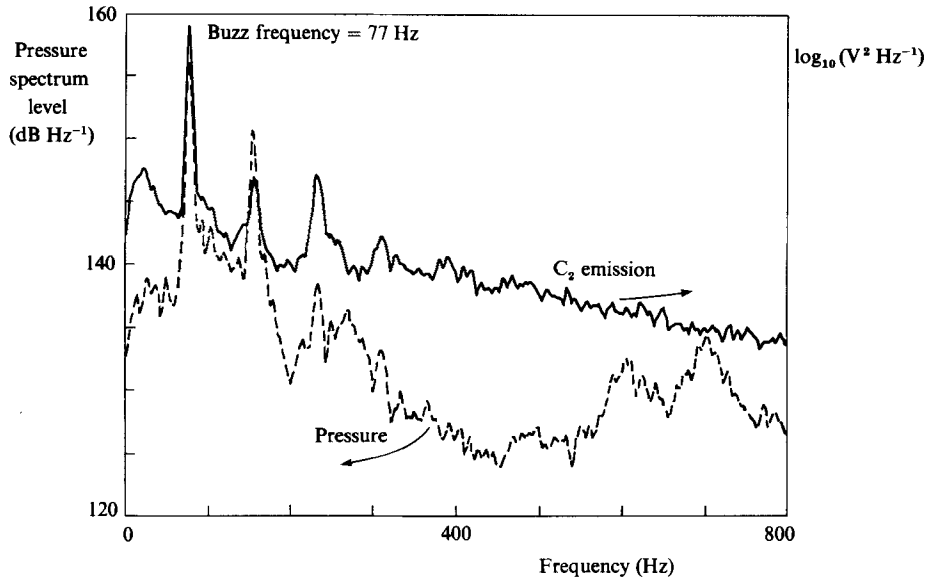

FIGURE 3. Example of each of pressure spectrum level (dashed) and power spectrum of C_2 emission (solid) at $x = 1.65$ m for configuration 1, $\phi = 0.70$.

Gaeltec. Relative errors between the magnitudes of the pressure fluctuation are better than $\pm 4\%$ of the measurement, and systematic errors in relative phase are of the order of 4° in the range 60–200 Hz.

4.2. *Velocity*

Mean and fluctuating velocities are measured upstream of the flame with a DISA 55D01 constant temperature hot-wire anemometer. The linearized output of the probe was calibrated in the rig or in the laboratory calibration tunnel against a pitot-static tube to an accuracy of $\pm 3\%$ of the amplitude of the fluctuation. Based on the manufacturers data, the phase relative to the pressure is known to better than 10° at frequencies of interest. Velocity measurements are made at approximately the centre of the duct.

4.3. *Heat release rate*

The emission of light from the major transitions of C_2 and CH radicals in a flame can depend on the location within the flame, the level of turbulence, the fuel to air ratio and the temperature (Gaydon 1974). Despite the number of possible variables, Hurle *et al.* (1968) have shown that the light emission from C_2 and CH radicals in the flame is linearly proportional to the volume flow rate of combustible mixture for open, premixed flames in laminar conditions and in low levels of turbulence. This implies that the C_2 or CH emission intensity is proportional to the heat release rate. Their deductions have subsequently been used, without further proof, as a measure of heat release rate (e.g. Price, Hurle & Sugden 1968; Shivashankara, Stahle & Handley 1975; Dines 1983; Ramachandra & Strahle 1983; Poinsot *et al.* 1987). Hurle *et al.* (1968) also discuss the behaviour of C_2 and CH emission at higher turbulence levels. In this regime, where the flame may not be properly stabilized and the combustion efficiency may be significantly less than 100%, the use of C_2 or CH radicals as a measure of heat release rate has not been directly confirmed. It therefore seemed prudent to check this proportionality for the conditions of our experiment.

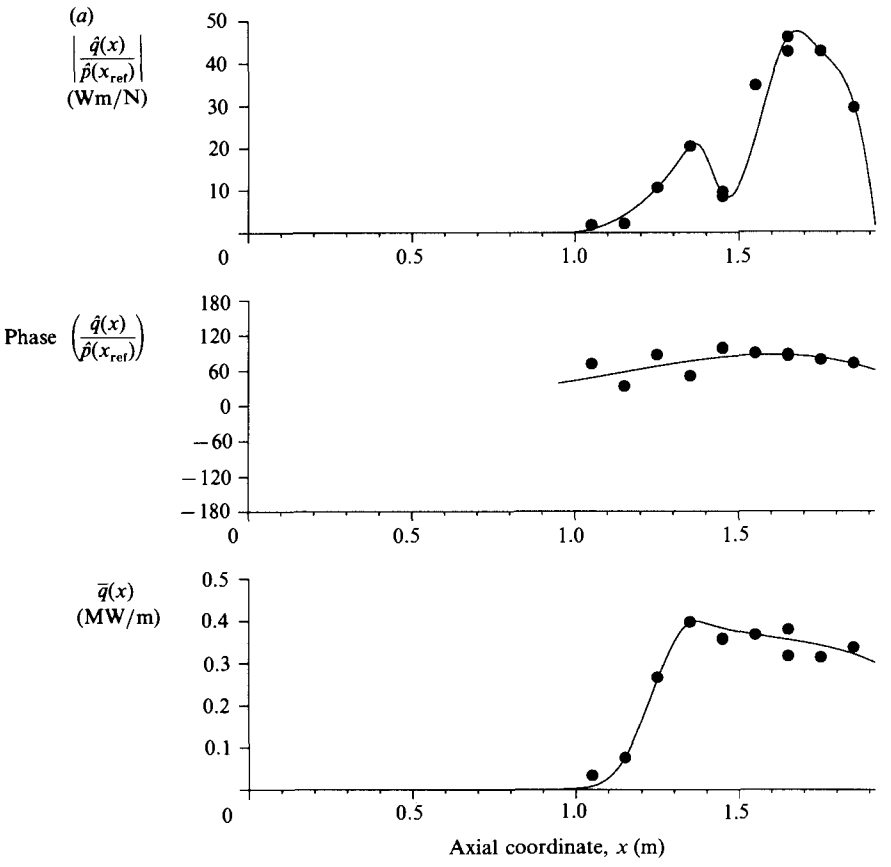

FIGURE 4(*a*). For caption see facing page.

Intensity of C_2 emission is measured at axial positions along the entire duct. We assume this is proportional to the distribution of heat release rate. In Part 2 the constant of proportionality is deduced from the measured exit temperatures. Least-squares cubic splines were fitted to the deduced mean heat release rate per unit length, $\bar{q}(x)$, and to the modulus and phase of the unsteady heat release rate per unit length, $\hat{q}(x)/\hat{p}(x_{ref})$, as shown in figure 4(*a*). Further it is shown in Part 2 that given the axial distribution of heat release rate, the equations of mass, momentum and energy conservation can be used to obtain the buzz frequency and growth rate and the mode shapes. The result of the computation is to predict the measured frequency within 1 Hz and to calculate the pressure distribution with excellent agreement to experimental data as shown in figure 4(*b*). C_2 emission intensity is thus a satisfactory measure of the distribution of heat release rate for an experiment at a given fuel to air ratio.

The optical arrangement for the measurement of C_2 emission is similar to that used in previous experiments. A screen blanks off all but a window in the flame. An image of this window is focused through a filter and remotely-operated shutter on to the photocathode of a photomultiplier. This is mounted in a light-tight box sufficiently far from the rig for the lens to subtend the same solid angle from all parts of the flame window. The peak transmission of the filter is at 516.7 nm (bandwidth 3.2 nm) close to the main C_2 transition. Since the bandwidth is degraded if the pencil of light

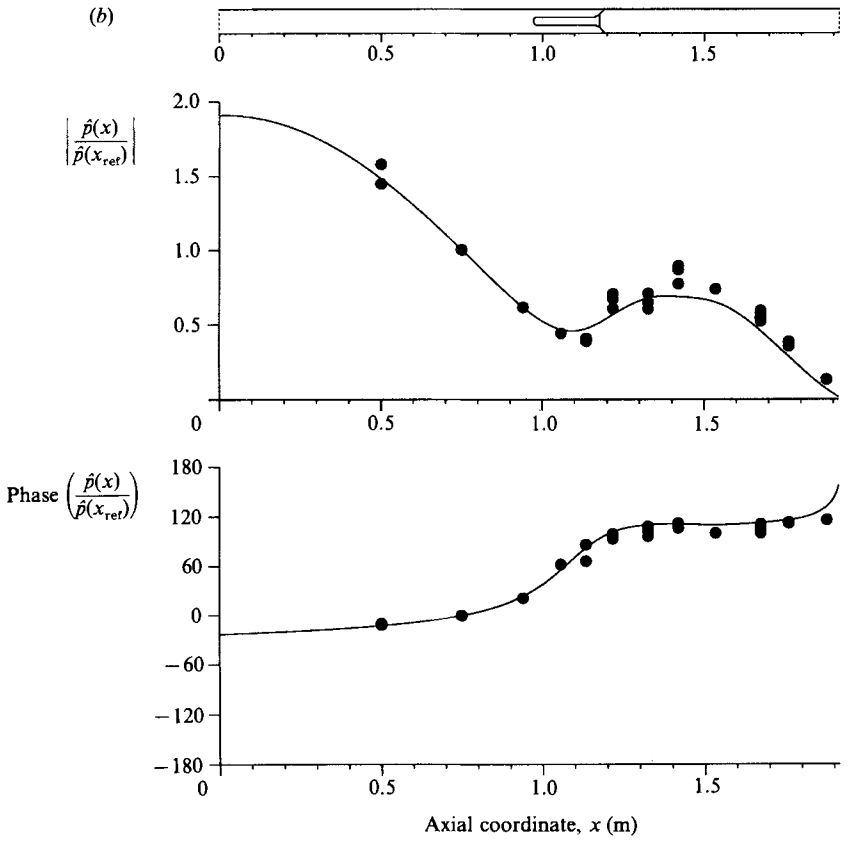

FIGURE 4. (*a*) Mean and unsteady heat release rates per unit length at the buzz frequency for configuration 1, $\phi = 0.70$. ●, experimental points; ——, spline fit. (*b*) Pressure variation along the duct at the buzz frequency for configuration 1, $\phi = 0.70$. ●, experimental points; ——, calculated using the spline fit to the heat release data.

entering the filter is more than a few degrees from the normal, an aperture stop is also required. The output of the photomultiplier, denoted by $I(x,t)$, is then assigned to the axial position of the centre of the window. The use of windowing to obtain C_2 emission intensity per unit length is justified by the linearity of $\bar{I}(x)$ with window length and by the insensitivity of the phase of $\hat{I}(x)$ to changes in window length. The light emission is integrated radially and over the window length so that events are low-pass filtered at a frequency given by the ratio of the event velocity to the window length. The response of the photomultiplier may be regarded as instantaneous at the frequencies under investigation.

In order to collect C_2 emission intensity data at all axial positions along the duct, a given set of mean flow conditions must be repeated. An experiment is then characterized by the averages of these conditions over a number of runs. The reproducibility of individual experimental runs is therefore crucial. The data of figure 4, collected over a two-month period, indicate that the drift in the reproducibility of the apparatus is satisfactory.

Duct diameter, $D = 0.070$ m
Gutter diameter, $d = 0.035$ m
Gutter blockage ratio = 25%
Inlet temperature = 288 ± 5 K

Configuration	Gutter lip position x_G (m)	Duct length L (m)	Reference position x_{ref} (m)	Inlet Mach number $\bar{M}_u$	Equivalence ratio ϕ	Buzz frequency f (Hz)
1	1.18	1.92	0.75	0.08	0.703 ± 0.005	77.1 ± 1.4
					0.670 ± 0.001	71.9 ± 0.9
					0.700 ± 0.001	80.1 ± 1.0
2	0.74	1.48	0.49	0.08	0.633 ± 0.006	73.2 ± 1.5
					0.643 ± 0.001	76.1 ± 0.8
					0.652 ± 0.001	81.2 ± 1.6
					0.664 ± 0.002	101.0 ± 1.2
					0.664 ± 0.003	102.9 ± 1.2
					0.702 ± 0.002	112.0 ± 1.2
3	1.19	2.18	0.76	0.08	0.652 ± 0.002	76.6 ± 0.4
4	1.18	1.92	0.75	0.15	0.708 ± 0.007	109.3 ± 1.3

TABLE 1

5. Description of experimental results

The experiments performed on the rig were designed to test the theory described in Part 2 and have examined the effect of the following with respect to a reference case.

(i) a 50% change in duct length upstream of the gutter,
(ii) a change of 10% in ϕ in steps of about 2%,
(iii) a 25% change in duct length downstream of the gutter,
(iv) a doubling of inlet Mach number.

Table 1 lists the geometry, mean running conditions, buzz frequencies and associated standard deviations in these experiments. The theory of Part 2 deals with small, linear perturbations so that we are interested in the onset of instability. There has therefore been no attempt to mark out the flammability and stability limits of the rig. However for the 10% change in ϕ in configuration 2, an examination of the buzz frequency and pressure band level (PBL) within 3 dB of the buzz frequency yields results which are consistent with those reported previously for lean mixtures (Sivasegaram & Whitelaw 1987). Both frequency and PBL increase slowly with ϕ on either side of a transition point, in this case $\phi = 0.65$, where the slope steepens considerably (figure 5*a*, *b*). We observe that the transition is also associated with a change in the axial distribution of C_2 emission per unit length, $i(x)$. For fuel to air ratios below transition (see for example figure 6*a*), the phase of $\hat{i}(x)/\hat{p}(x_{ref})$ varies linearly with axial distance in a manner reminiscent of the convection of a hot spot with a velocity of approximately 30 m s^{-1} along most of the duct. We refer to this as convecting behaviour. In this the data are similar to those described in Part 2 during the forced excitation of a critically stable flame. As expected, the slope becomes more gradual as the gases accelerate towards the end of the duct and there the C_2 emission is nearly in phase with the pressure perturbations. Because the phase of the pressure is almost constant in the flame, there will be alternating regions of driving and damping and the amplitude of the buzz is relatively low. If convecting behaviour

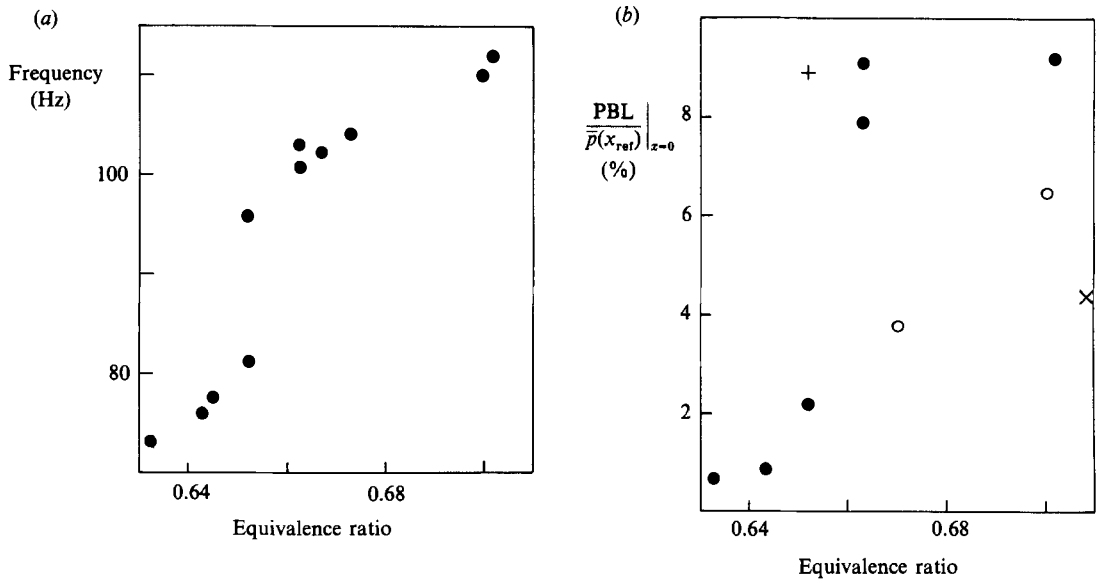

FIGURE 5. (*a*) Dependence of fundamental frequency on equivalence ratio for configuration 2. (*b*) Dependence of pressure band level (PBL) within 3 dB of the buzz frequency on equivalence ratio. The PBL is that at the choked restriction, $x = 0$, and is found from the measured pressure at x_{ref} and the mode shape predicted assuming a choked, upstream boundary condition. It is normalized by the mean pressure at x_{ref}. ○, configuration 1; ●, configuration 2; +, configuration 3; ×, configuration 4.

exists along most of the duct we therefore have weak buzz. Convection of wrinkles with the mean unburned gas velocity has previously been reported for both naturally and artificially produced disturbances on an open burner (Snellink 1973) and for a confined, turbulent flame (Yoshida & Tsuji 1984), although the mechanism of formation and scale of the instability in the latter study is quite different to the present case. Similar descriptions have been used to explain the axial distribution of the phase of light emission in a dump combustor (Hedge *et al.* 1987), where the speed was again found to increase slowly downstream. In all these cases the inlet velocity was very much less than in the present experiments.

In contrast, for $\phi = 0.66$ (figure 6*b*) and above, this convecting behaviour extends only a short distance beyond the gutter lip. A second type of behaviour, which we term concurrent behaviour, occupies the greater portion of the duct. Cine film of this shows that the flame alternately fills the duct then contracts, leaving only a kernel of flame on the gutter. Here, the phase of the unsteady C_2 emission assumes an almost constant value close to that of the pressure. For values of ϕ exceeding the transition value then, Rayleigh's criterion states that conditions are favourable for a large energy input to the instability over a large portion of the duct, resulting in what we call established buzz. There is therefore an increase in $\mathrm{PBL}/\overline{p}|_{x=0}$ (see figure 5*b*) from 0.7 % at $\phi = 0.63$ to 9.2 % at $\phi = 0.70$.

Sivasegaram & Whitelaw (1987) describe the presence of two frequencies in their pressure spectra at values of ϕ where the frequency is observed to rise steeply. They attribute this observation to the simultaneous presence of a vortex-shedding frequency associated with a Strouhal number of 0.2–0.35 and an acoustic quarter-wave frequency associated with the length upstream of the flame holder. Power spectra of C_2 emission along the duct at $\phi = 0.65$ in our experiments (Figure 7) also

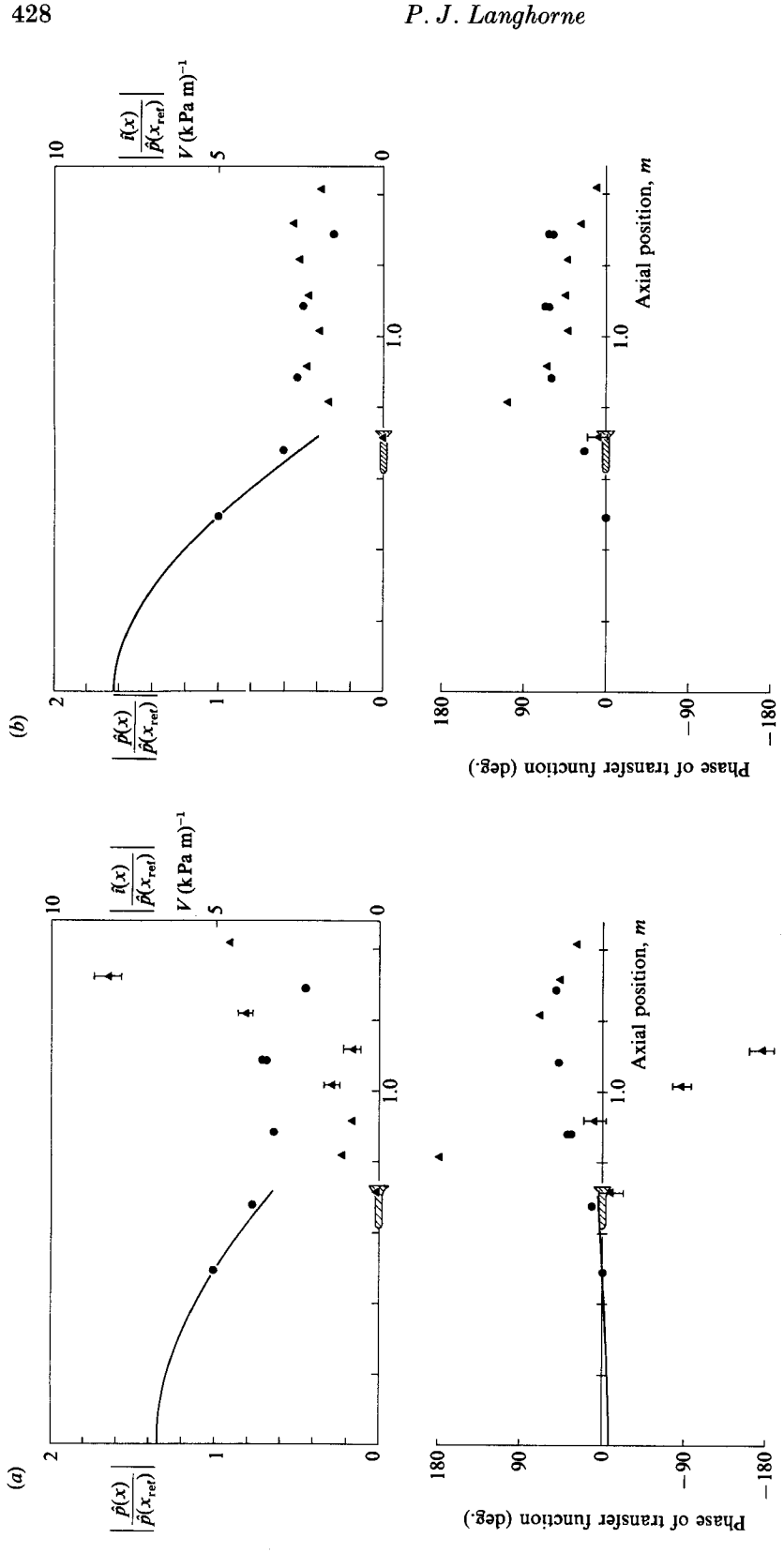

FIGURE 6. (*a*) Modulus and phase of the transfer function at the buzz frequency (81 Hz) as a function of axial position. $\phi = 0.65, \bar{M}_u = 0.08$ in configuration 2. ●, pressure; ▲, C_2 emission. Solid curve is the mode shape of the pressure upstream of the flame holder, deduced from the reflection of an acoustic wave at the measured frequency from the choked inlet restriction. 95 % confidence intervals for the true modulus and phase are shown by error bars where they are larger than the symbol size. (*b*) Modulus and phase of the transfer function at the buzz frequency (101 Hz) as a function of axial position. $\phi = 0.66, \bar{M}_u = 0.08$ in configuration 2. ●, pressure; ▲, C_2 emission.

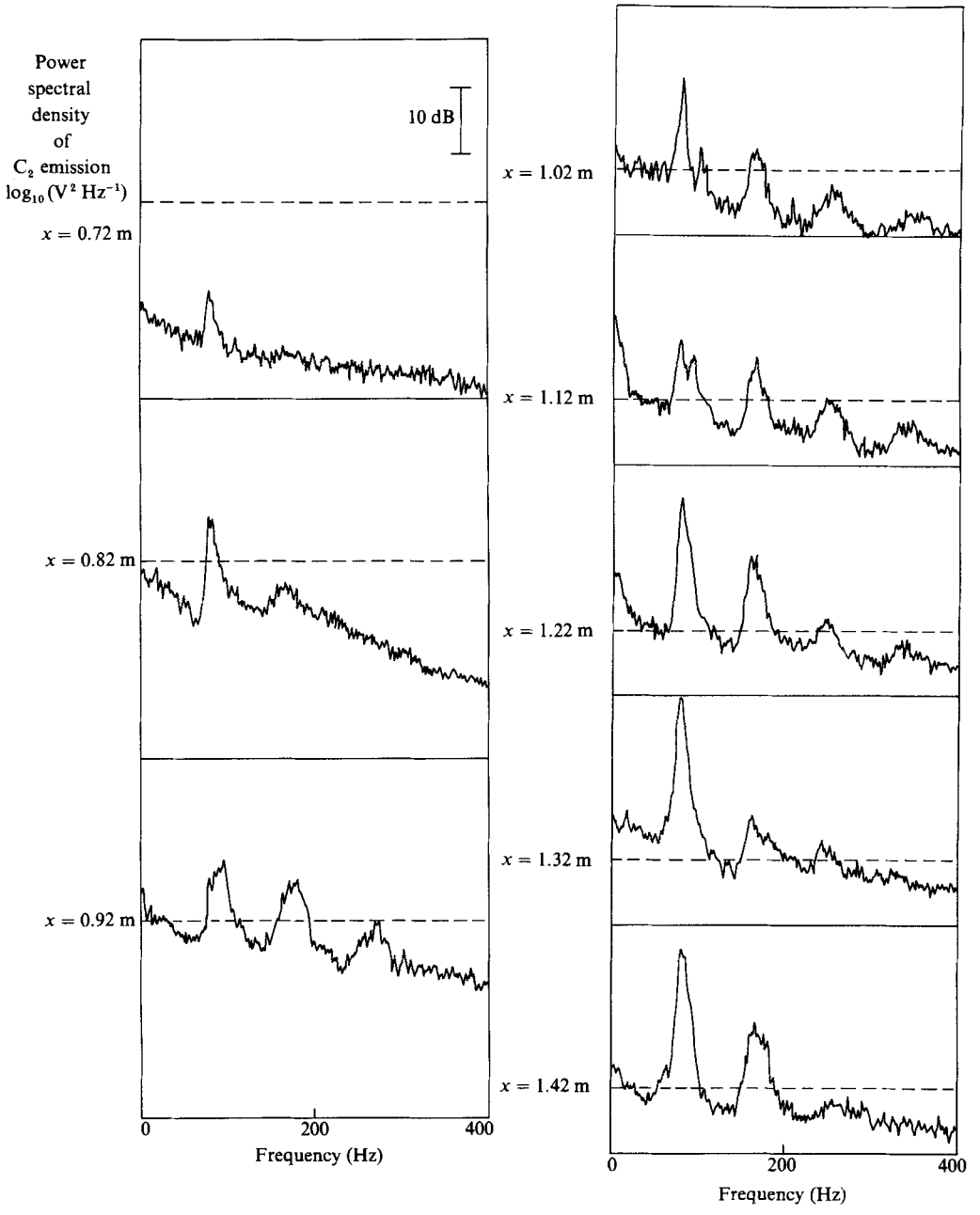

FIGURE 7. Power spectra of C_2 emission at axial positions, x, for $\phi = 0.65$ in configuration 2. The upper bound is the same in all plots and 10 dB is shown. The reference level (shown dashed) is also the same at all axial positions.

show the presence of a double peak at $x = 1.02$ m and $x = 1.12$ m. Although this observation is similar to that of Sivasegaram & Whitelaw, our interpretation differs. The dominant frequency in the pipe is determined by the integrated effect of the interaction between the unsteady pressure and heat release rate throughout the duct. We have seen that two modes of coupling are possible and the resulting buzz

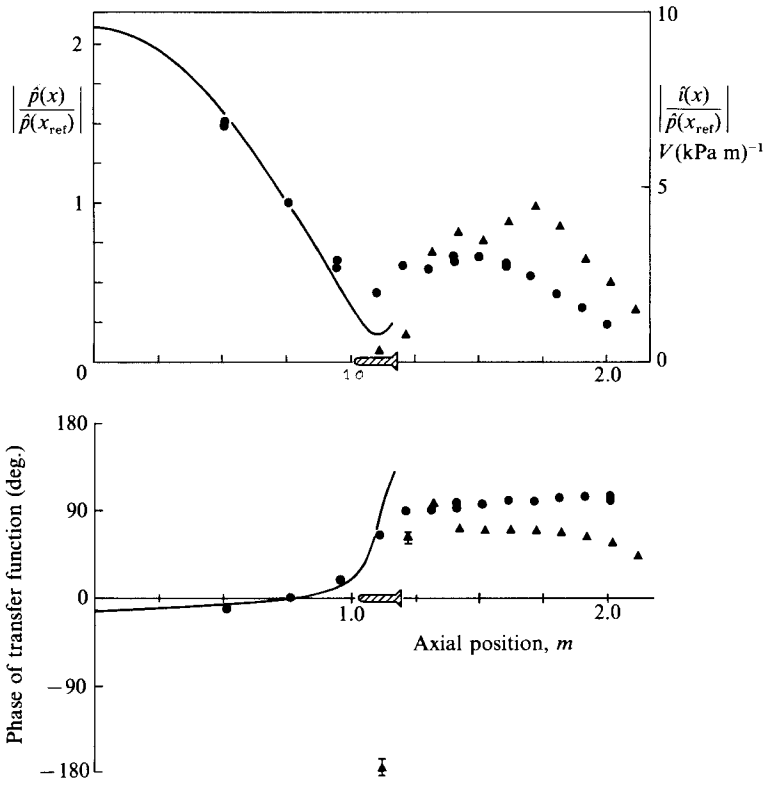

FIGURE 8. Modulus and phase of the transfer function at the buzz frequency (77 Hz) as a function of axial position. $\phi = 0.65, \bar{M}_u = 0.08$ in configuration 3. ●, pressure; ▲, C_2 emission. Solid curve is the mode shape of the pressure upstream of the flame holder, deduced from the reflection of an acoustic wave at the measured frequency from the choked inlet restriction. 95% confidence intervals for the true modulus and phase are shown by error bars where they are larger than the symbol size.

frequency depends on which occurs. At the transition from weak to established buzz, random fluctuations will cause the system to flip between modes. Thus, when averaged in time, both frequencies will be present.

Having identified two possible types of behaviour it is interesting to investigate how their existence is influenced by changes in geometry and Mach number. Configurations 3 and 4 were studied with this purpose. Configuration 3 was performed at a value of ϕ which would have produced weak buzz in configuration 1. However the significant lengthening of the combustion zone caused the phase of the C_2 emission to be constant and close to that of the pressure along almost all the duct (see figure 8), resulting in the high level of the pressure fluctuations near the choked inlet (figure 5*b*). In this configuration weak buzz never occurred. The propensity for buzz was so great that when ϕ was reduced, a flame could no longer be stabilized in the presence of the violent oscillations in velocity. This inability to stabilize a flame has also been observed by Yamaguchi, Ohiwa & Hasegawa (1985) and Schadow *et al.* (1987). We were therefore unable to investigate any values of ϕ which might produce weak buzz in this geometry.

At the higher Mach number in configuration 4 the operating range of the buzz rig was again greatly reduced. At $\phi = 0.65$ and below, no peak was observed above the

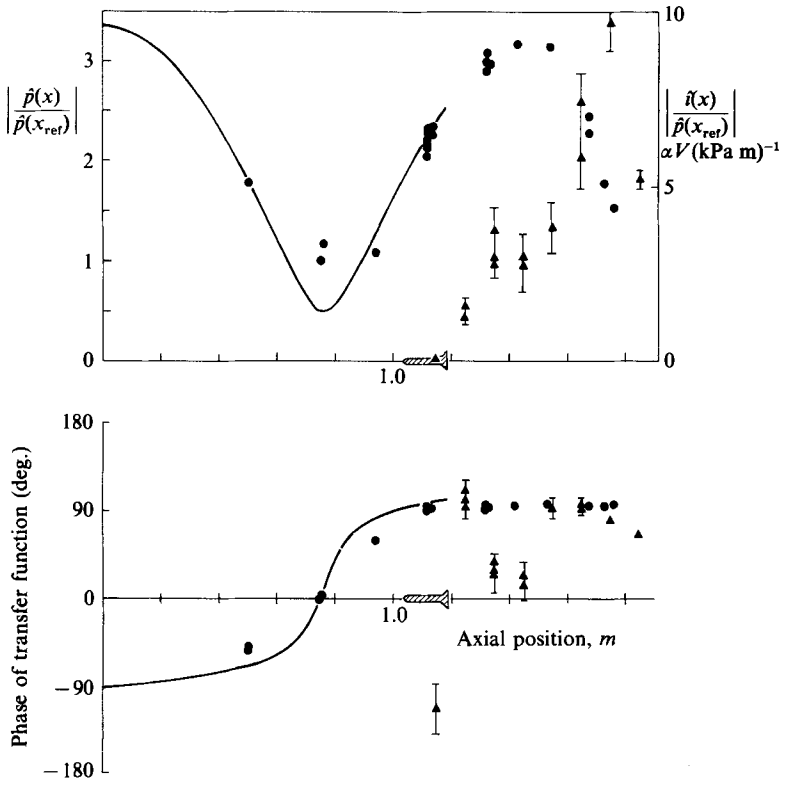

FIGURE 9. Modulus and phase of the transfer function at the buzz frequency (109 Hz) as a function of axial position. The gain of the photomultiplier has been changed by a factor α due to the higher light levels. $\phi = 0.71, \bar{M}_u = 0.15$ in configuration 4. ●, pressure; ▲, C_2 emission. Solid curve is the mode shape of the pressure upstream of the flame holder, deduced from the reflection of an acoustic wave at the measured frequency from the choked inlet restriction. 95% confidence intervals for the true modulus and phase are shown by error bars where they are larger than the symbol size.

broadband combustion noise, while a significant increase in ϕ caused sporadic, large-amplitude events which caused blowoff. Consequently at the equivalence ratio presented, the coherence between $i'(x,t)$ and $p'(x,t)$ was lower than in the other experiments and errors in the modulus and phase are therefore higher (see figure 9). The geometry and ϕ are comparable with configuration 1 and comparison with these experiments (figures 4 and 11) shows that the increase in approach speed has extended the region of convecting behaviour to occupy approximately half of the combustion zone. As a result $\mathrm{PBL}/\bar{p}|_{x=0}$ at the buzz frequency in figure 5(*b*) is seen to be lower than for configuration 1.

Configuration 4 is interesting for two reasons. First the data presented for a Mach number of 0.08 in figures 4, 6 and 8 would seem to confirm the observations of Heitor *et al.* (1984) in that the acoustic mode is simply a quarter wave in the cold portion of the duct. As shown in figure 9, the experiment at a Mach number of 0.15 is a counter-example to this simple description. Secondly, unlike many previous experiments with very low inlet velocities, this is a condition of some practical interest to afterburner design and it is therefore crucially important that any theory should be able to reproduce trends in this data.

Summarizing the description of the axial distribution of $\hat{i}(x)/\hat{p}(x_{\mathrm{ref}})$ at the buzz

frequency we make the following obervations. At all flow conditions there is a region just downstream of the gutter lip in which fluctuations in C_2 emission intensity convect along the duct at approximately the speed of the cold fluid. Further downstream the phase of the C_2 emission assumes a value close to that of the unsteady pressure. The axial position at which the transition between these two types of behaviour takes place, and consequently which occupies the major portion of the duct, determines the frequency and ultimate magnitude of the instability.

6. Discussion

In §5 the convecting behaviour was readily explained as the convection of a fluctuation in C_2 emission with the speed of the cold fluid. However the fluid dynamics producing the observed phase of the C_2 emission in concurrent behaviour is less obvious. Two photomultipliers were therefore set up to study the evolution of the unsteady light between two neighbouring locations. In addition to providing this information, the output of these devices, once suitably adjusted to the same gain, gives a useful indication of the error in the light emission results. Although the optical filters were nominally identical (peak transmission at 516.7 nm, bandwidth 3.2 nm compared with 518.0 nm, bandwidth 3.6 nm) the results were found to depend on the exact position of maximum transmission. Nonetheless figures 10 and 11 show the reproducibility of the C_2 emission intensity, which is satisfactory for our purposes.

Experiments were performed with the dual photomultiplier system at two equivalence ratios. One example exhibited weak buzz at $\phi = 0.67$, while the other showed the characteristics of established buzz at $\phi = 0.70$ (both in configuration 1). These statements are illustrated in the plots of mean and unsteady C_2 emission in figures 10 and 11 respectively. Samples of time series of light emission from 75 mm long windows, centred at locations half a window width downstream of the gutter lip (position A) and 150 mm downstream of this (position B), are also given in figure 11. These data lie within the convecting region for both examples and in both cases fluctuations in C_2 emission are seen to be amplified as they are convected downstream. In addition, the data at the higher amplitudes ($\phi = 0.70$) intermittantly display distinct troughs dipping far beneath the ambient level. However at positions C and D, the character of the light emission has changed markedly with the 0.03 increase in ϕ; for the weak buzz ($\phi = 0.67$), the wave-form at C is amplified and convected downstream to D approximately 3 to 4 ms later. On the other hand the data for established buzz ($\phi = 0.70$) show that the reaction at the upstream location C commences before that at the location D downstream, but that it is extinguished at C at approximately the same time or slightly after that at D. We suggest this narrowing of the reaction pulse is due to the consumption of available gas by the intense combustion. The leading edge of the reaction event was in fact found to be travelling at approximately the radially-averaged velocity in the combustion zone. However, since the pulse is of shorter duration at large values of x, the reason for the small change in phase with axial position is clear. Without further evidence we cannot, of course, tell whether the low levels of C_2 emission correspond to burnt or unburnt gas or to some combination of these. We would expect temperature data to reflect the square-wave behaviour observed in the C_2 emission results. Such data have been reported on a similar rig by Smart, Jones & Jewell (1976) although they gave no explanation of the waveforms they measured.

It is obvious from the examples of the time series of C_2 emission that there will be

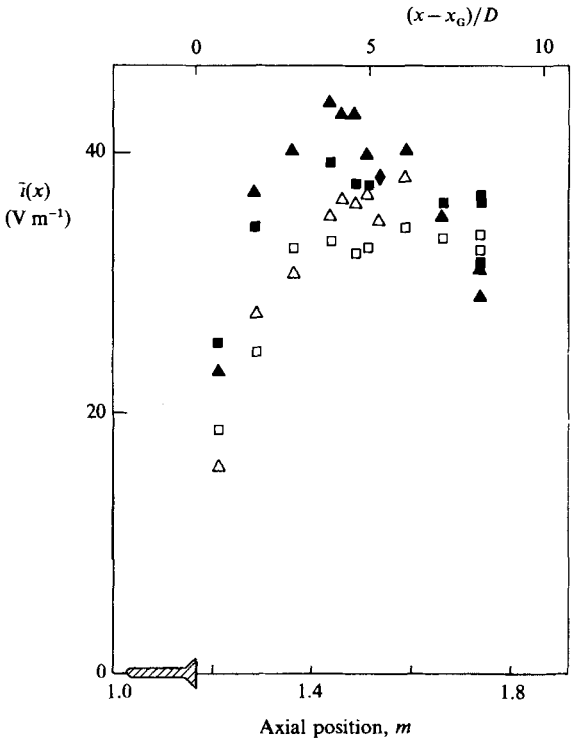

FIGURE 10. Mean C_2 emission per unit length as a function of axial position for configuration 1. Weak buzz is shown by open symbols, while filled symbols denote established buzz. △, photomultiplier 1 and □, photomultiplier 2, $\phi = 0.67$; ▲, photomultiplier 1 and ■, photomultiplier 2, $\phi = 0.70$.

a dramatic change in the axial distribution of the light between weak and established buzz. This is shown for both the mean C_2 emission per unit length in figures 10 and 12(*a*) and the square root of the spectral power within 3 dB of the buzz frequency (figure 12*b*) as ϕ is varied in configuration 2. In all cases the data for mean C_2 emission show a maximum within the length of the duct. Provided a change in ϕ does not produce a transition from weak to established buzz, an increase in ϕ simply increases the magnitude of $\bar{i}(x)$ and $|\hat{i}(x)|$ but not the axial distribution. However the maximum value is significantly closer to the gutter lip during established buzz. It should be noted that the distribution of unsteady C_2 emission roughly mimics the form of the mean, an observation which is used in the development of the model in Part 2. Further note that the experiment at $\phi = 0.66$ was repeated and C_2 emission intensity was found to be reproduced at all axial locations to better than 15% of the magnitude of the measurement. More importantly, features of the axial distribution are repeatable and may be regarded as significant.

The observed axial distributions of the mean and unsteady C_2 emission per unit length can be explained as follows. Figure 13 shows that the increase in the mean light emission along the duct is associated with weak behaviour; i.e. data points in the upper half plane have large and distributed negative values of the slope of the phase of the unsteady C_2 emission. Thus convecting behaviour is associated with an increase in mean C_2 emission with x, from a low value at the gutter lip. We tentatively suggest that this behaviour is associated with the radial spreading of a

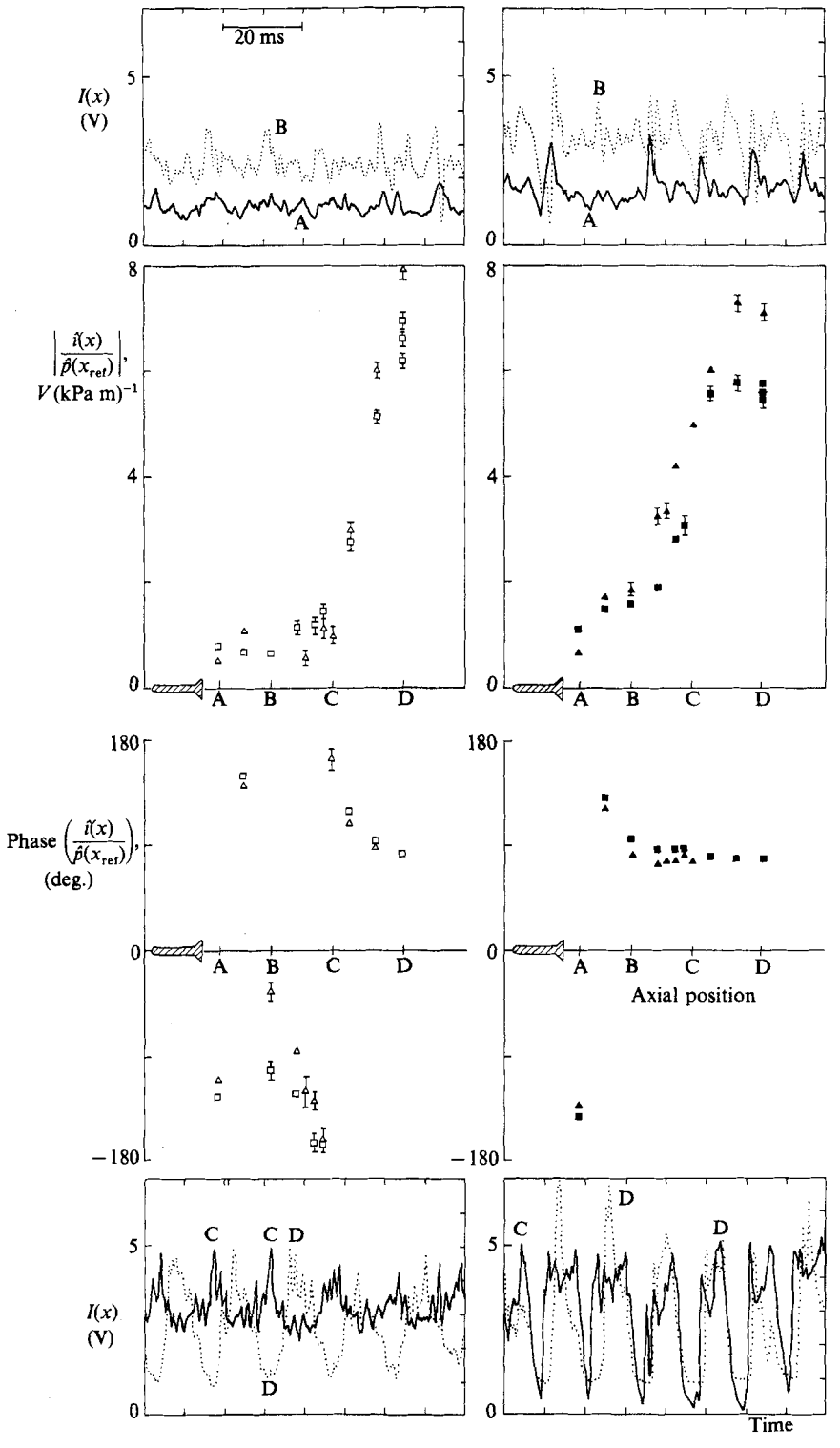

FIGURE 11. For caption see facing page.

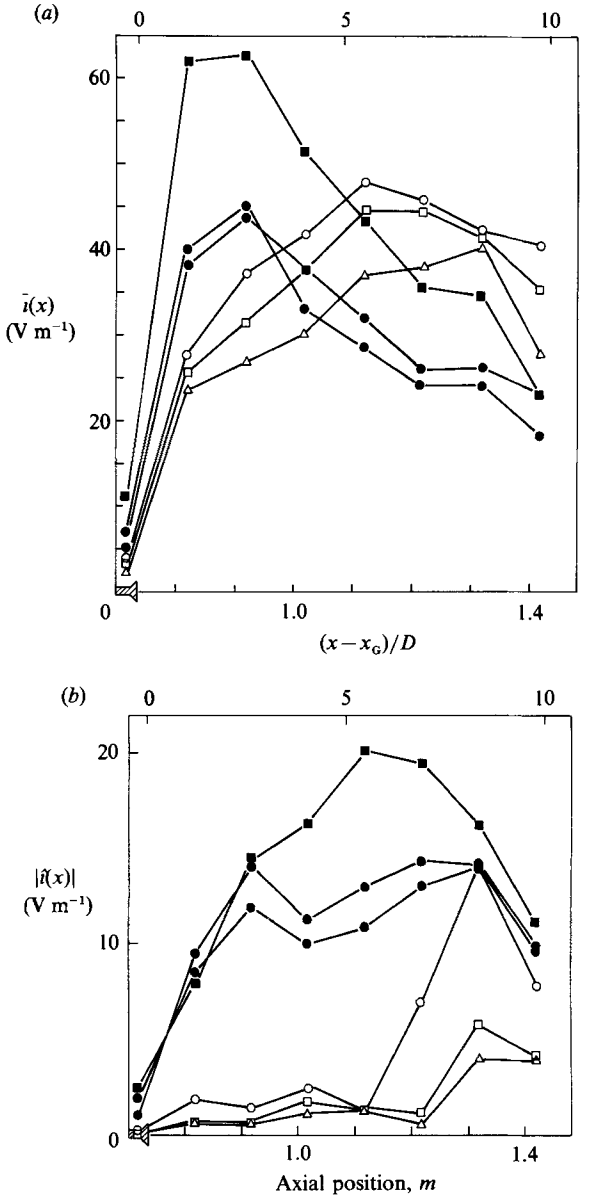

FIGURE 12. (*a*) Mean C_2 emission per unit length as a function of axial position for various values of ϕ in configuration 2. △, $\phi = 0.63$; □, $\phi = 0.64$; ○, $\phi = 0.65$; ●, $\phi = 0.66$; ■, $\phi = 0.70$. (*b*) Modulus of C_2 emission per unit length within 3 dB of the buzz frequency as a function of axial position for various values of ϕ in configuration 2. △, $\phi = 0.63$; □, $\phi = 0.64$; ○, $\phi = 0.65$; ●, $\phi = 0.66$; ■, $\phi = 0.70$.

FIGURE 11. Modulus and phase of C_2 emission at the buzz frequency as a function of axial position for configuration 1. Weak buzz is shown by open symbols, while filled symbols denote established buzz. △, photomultiplier 1 and □, photomultiplier 2, $\phi = 0.67$, buzz frequency = 72 Hz; ▲, photomultiplier 1 and ■, photomultiplier 2, $\phi = 0.70$, buzz frequency = 80 Hz. 95% confidence intervals for the true modulus and phase are shown by error bars where they are larger than the symbol size. Inserts show samples of time series of total C_2 emission, in volts, measured simultaneously at two windows centred on locations A to D. ——, upstream location; ·····, downstream location.

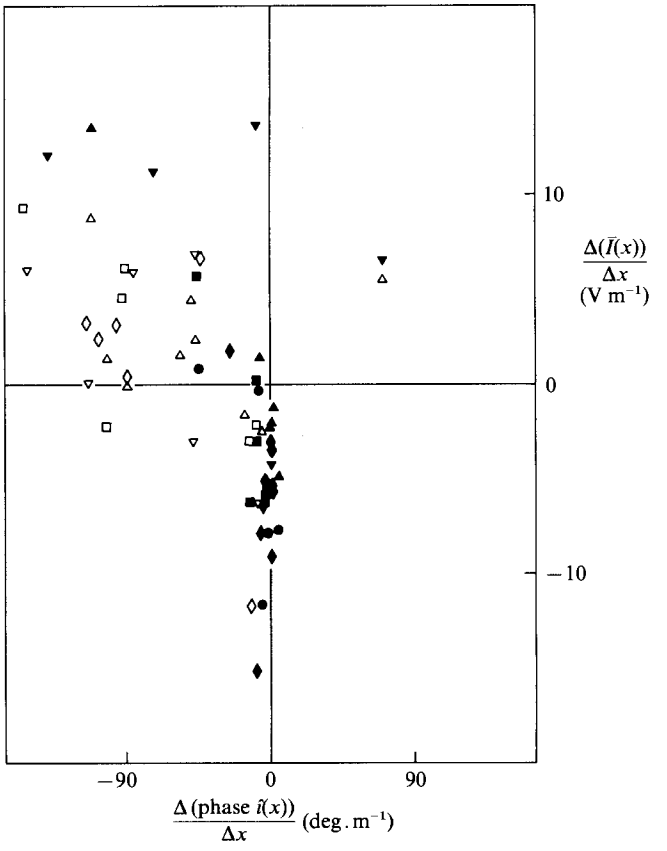

FIGURE 13. Rate of change of mean C_2 emission with axial position plotted against rate of change of phase of the unsteady C_2 emission at the buzz frequency with axial position. Weak buzz is shown by open symbols while established buzz is denoted by filled symbols. △, configuration 1, $\phi = 0.67$; ▲, configuration 1, $\phi = 0.70$; ◇, configuration 2, $\phi = 0.63$; ▽, configuration 2, $\phi = 0.64$; □, configuration 2, $\phi = 0.65$; ■, configuration 2, $\phi = 0.66$; ●, configuration 2, $\phi = 0.70$; ◆, configuration 3, $\phi = 0.65$; ▼, configuration 4, $\phi = 0.71$.

conical ignition front from the gutter. Since the angle of the cone is small, fluctuations propagate along this front at approximately the speed of the reactants. In this region of convecting behaviour the magnitude of the unsteady C_2 emission per unit length is low. We suggest that the maximum in the mean C_2 emission per unit length occurs at the time-averaged position of flame impingement on the wall where the mean flame area is maximum.

Downstream of the maximum in the mean C_2 emission, the slope of $\bar{I}(x)$ is negative. We see in figure 13 that the lower half plane corresponds to regions of constant phase in the unsteady light signal. Thus the reduction in $\bar{I}(x)$ with axial position is associated with concurrent behaviour. Beyond the position of maximum, mean light emission, the combustion is intermittantly detached from the gutter. This conjecture is supported by our cine film. The source of ignition is now a kernel of flame which remains attached to the stabilizer. In this region we suggest the flame is stretched significantly by fluctuations in the oncoming flow which distort the flame front causing it to break down into pockets of burnt and unburnt gas. The effect of an increase in the magnitude of the instability at fixed x or of an increase in axial

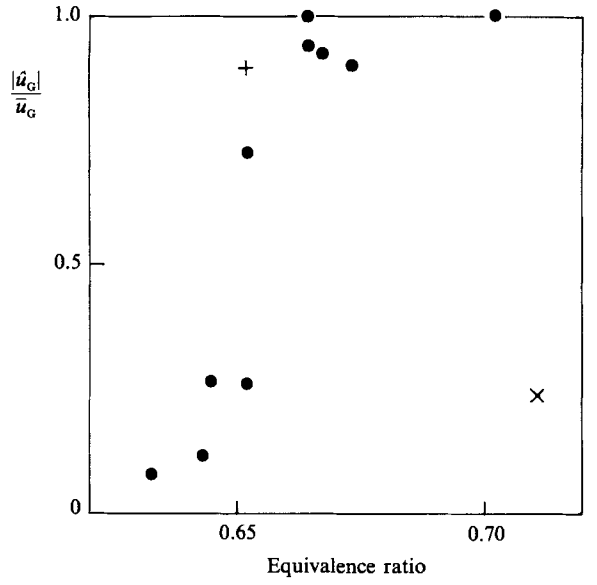

FIGURE 14. Peak amplitude of the component of velocity within 3 dB of the buzz frequency, extrapolated to the gutter lip and normalized by the mean velocity there. This is plotted as a function of ϕ for configuration 2, ●; configuration 3, +; and configuration 4, ×.

position at fixed ϕ is then for the reaction to be 'off' for an increasingly large fraction of the cycle as shown in figure 11 at positions C and D. Thus in concurrent behaviour the measured mean value of C_2 emission decreases with axial position. The existence of weak or established buzz in the duct is entirely determined by the position where the mean flame area is maximum.

Figures 12(*a*) and 12(*b*) show that the unsteady C_2 emission can be a significant fraction of the mean. We have seen that fractional oscillations in pressure are much less than this. However since the approach Mach number is low, velocity fluctuations which are a significant fraction of the mean are possible. The peak amplitude of the component of axial velocity within 3 dB of the buzz frequency, $|\hat{u}(x)|$ was measured at an upstream location. This was then multiplied by a ratio calculated from the upstream boundary condition to give $|\hat{u}_G|$ at the gutter lip. In figure 14 this is normalized by the mean velocity, $\bar{u}_G$, in the cold flow at the gutter lip. The figure shows that, at the higher values of ϕ, low velocities and even flow reversal occurred periodically in the cycle. Further evidence of reversal was clearly visible in velocity records. For configuration 2 the transition at $\phi = 0.65$ from weak to established buzz is accompanied by an increase in $|\hat{u}_G|/\bar{u}_G$. This then reduces the turbulent mixing time resulting in the observed behaviour of the mean C_2 emission which has a maximum close to the gutter lip (see figure 12*b*). In the same way the pattern of the mean C_2 emission per unit length is determined by the magnitude of $|\hat{u}_G|/\bar{u}_G$ for configurations 3 and 4.

The probability of transitory excursions of the flame behind the gutter lip during a cycle of buzz is deduced from light measurements centred on a window just upstream of the gutter lip for configuration 2. When the fractional velocity is less than 0.5 the probability is approximately zero. For a fractional velocity greater than 0.5, the probability is found to rise rapidly with $|\hat{u}_G|/\bar{u}_G$. We use this result and the small values of fractional velocity measured for configuration 4 to deduce that the flame movement at higher inlet velocities is confined to regions downstream of

the stabilizer. Since $\mathrm{PBL}/\bar{p}|_{x=0} \sim 4\%$ for this experiment, we may deduce that large movements of the flame are not necessary for the generation of significant pressure fluctuations. However even when $|\hat{u}_G|/\bar{u}_G$ is close to unity, the flame travels upstream of its holder only about once in every five cycles demonstrating the large cycle to cycle variations associated with established buzz.

We now know that large values of the fractional velocity at the gutter lip are associated with the square-wave type behaviour in the time series of C_2 emission. In an attempt to form a clearer picture of the light emission in weak and established buzz we examine phase averaged contours of total C_2 emission from 0.1 m windows, $\bar{I}+I'$. These are drawn as a function of non-dimensionalized position and time. Position is measured relative to the gutter lip and is non-dimensionalized with respect to duct diameter, i.e. $(x-x_G)/D$, while time is non-dimensionalized with respect to a buzz period, t/T. We have seen that $|\hat{u}_G|/\bar{u}_G$ can be of order 1.0 whereas $\mathrm{PBL}/\bar{p} \sim 0.1$ and thus zero time is arbitrarily taken as the maximum in the unsteady velocity at the gutter lip. Examples of data illustrating weak buzz at $\phi = 0.65$ (figure 15*a*) and established buzz at $\phi = 0.66$ (figure 15*b*) are shown for configuration 2. The slope of the contours in figure 15(*a*) indicate convection speeds of the order of 27 m s^{-1} until the acceleration at $(x-x_G)/D = 6$ and transition to large fluctuations in C_2 emission. For the established buzz (figure 15*b*) the sharp rise in C_2 emission takes place at smaller values of $(x-x_G)/D$. This information is rapidly convected downstream and, after a period of intense combustion, there is almost simultaneous extinction at all axial locations throughout the duct. The residence time of the gases in the duct is less than the time for the gases to react and combustion extends well beyond the end of the duct. The confined heat release is less than for weak buzz and consequently the mean upstream pressure was lower in the intense oscillations at $\phi = 0.66$. It can be seen in figure 15(*b*) that at $t/T \sim 0.1$, light levels are low throughout the duct with a trough five gutter diameters, d, from the stabilizer at $(x-x_G)/D = 2.5$. This is just upstream of the end of the recirculation zone at $6d$ to $7d$ ($(x-x_G)/D = 3.5$) (Zukoski 1978; Yamaguchi *et al.* 1985). The feature is similar to the constriction described by Yamaguchi *et al.* (1985), which virtually splits the flame in two parts at the end of the recirculation zone, after having moved downstream from the flame holder. Our data implies that, after relative extinction throughout the duct at $t/T \sim 0.8$, a kernel of flame which has been shielded by the gutter acts as a source of ignition for the following cycle at $t/T \sim 0.1$ in a similar manner to the behaviour of a pulsating combustor (Reuter *et al.* 1986).

The instantaneous pressure gradient, deduced from the calculations in Part 2 and scaled by the measured pressure fluctuation, is plotted at quarter cycle integrals as a function of axial position for an example of established buzz in figure 16. C_2 emission at these instants is also shown. The most distinctive feature of these results is the reversal of sign close to the gutter lip during established buzz (figure 16).

Let us consider a cycle of established buzz. Begin at $t/T = 0$ in figures 15(*b*) and 16 when there is a maximum in the unsteady velocity at the gutter lip. Close to the gutter lip fluctuations in C_2 emission travel along the conical flame front at a speed close to that of the velocity of the reactants because of the small angle of the flame to the flow. This extends as far as a position where the pressure and light fluctuations are in phase and where the mean and unsteady C_2 emission are sufficiently large. The axial position at which these requirements are satisfied will depend on the chemical delay time (or ϕ) and the turbulent mixing time. Beyond this point, i.e. $(x-x_G)/D \sim 0.15$ in figure 15(*b*), energy is fed into the instability. The flame front can no longer be described as a continuous entity and the excess mass of combustible

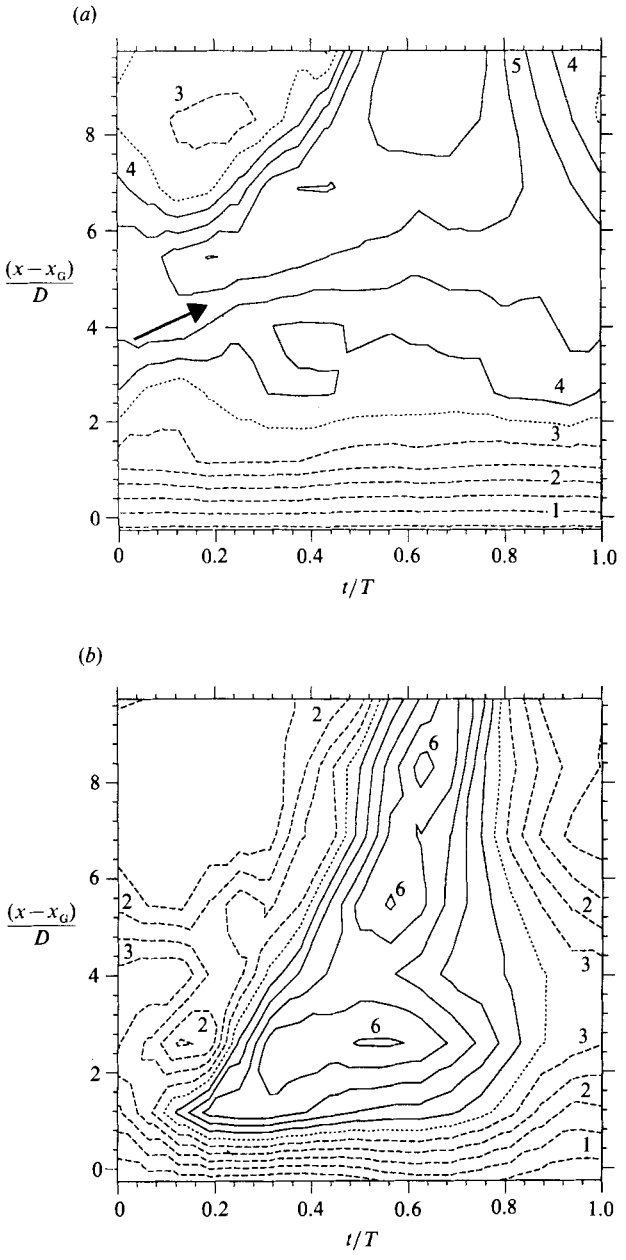

FIGURE 15. Contours, in volts, of the magnitude of the C_2 emission from 0.1 m windows as a function of axial position in duct diameters, D, downstream of the gutter lip and of time non-dimensionalized by buzz period, T. $t/T = 0$ corresponds to the maximum velocity at the gutter lip. The arrow shows the contour slope for an event travelling at 30 m s^{-1}. (*a*) configuration 2, $\phi = 0.65$, buzz frequency = 81 Hz, $T = 12.3$ ms. (*b*) configuration 2, $\phi = 0.66$, buzz frequency = 101 Hz, $T = 9.9$ ms. – – –, contours for output < 3.5 V; ——, contours for output > 3.5 V; - - - - -, contours at 3.5 V.

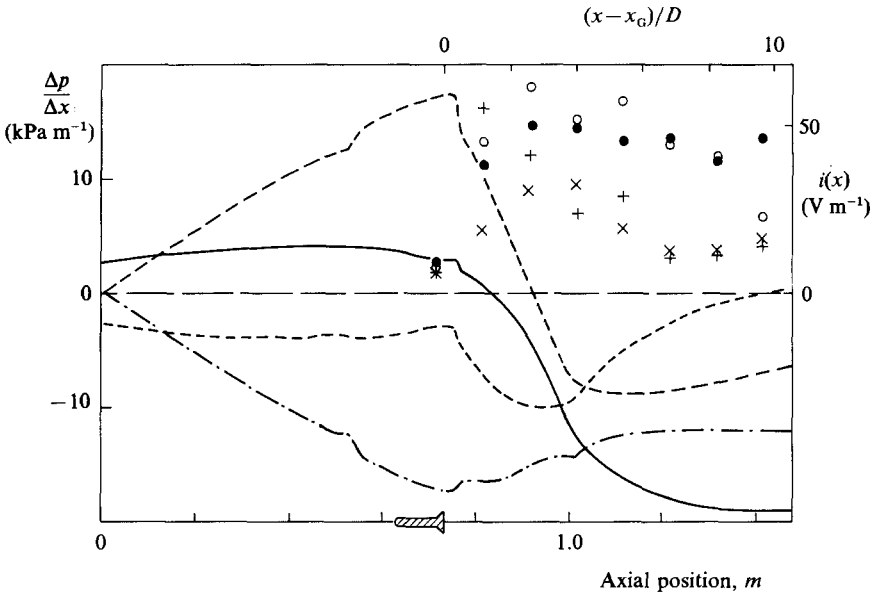

FIGURE 16. Plot of pressure gradient and C_2 emission per unit length as a function of axial position at quarter-period intervals. $t/T = 0$ is taken as the instant of maximum unsteady velocity at the gutter lip. Configuration 2 at $\phi = 0.66$, established buzz. Symbols shown C_2 emission while curves are pressure gradient. × and ----, $t/T = 0$; + and − − −, $t/T = 0.25$; ○ and ——, $t/T = 0.50$; ● and ——, $t/T = 0.75$.

mixture discharged into the flame at $t/T = 0$ burns rapidly as it is convected downstream at approximately the local radially-averaged gas velocity. This produces a large negative pressure gradient in the combustion zone from $t/T = 0.25$ to $t/T = 0.5$ which accelerates the products. Because $p'(L, t) = 0$ at the exit, $x = L$, the pressure at the gutter lip is raised, reducing the velocity there to its minimum at $t/T \sim 0.5$. The slug of mixture discharged at $t/T = 0$ is consumed with some of the combustion taking place outside the duct. By $t/T \sim 0.5$ the gutter lip velocity has reached a minimum and the burnt material is not replenished so that the reaction is extinguished at $t/T \sim 0.8$. There is thus a reduction in the accelerating pressure gradient along the combustion zone from $t/T = 0.75$ to 1.0 and an acceleration of gases across the gutter lip. Provided a kernel of flame has managed to cling to the gutter wake to act as the ignition source, the cycle is restarted.

7. Conclusions

(i) Two forms of interaction between a reaction zone and sound field have been identified. We have called one convecting behaviour and the other concurrent.

Convecting behaviour. The perturbation in the unsteady C_2 emission travels along the duct with a velocity close to that of the reactants. The phase of the C_2 emission then varies linearly with respect to that of the pressure and, according to Rayleigh's criterion, there are alternating regions of driving and damping.

Concurrent behaviour. Time series plots of C_2 emission take the approximate form of a square-wave. The leading edge of the reaction travels with a velocity close to the local, radially-averaged mean of the hot and cold gas. The duration of the pulse decreases downstream due to consumption of the reactants by the intense

combustion. As a result, the phase of the C_2 emission is approximately constant and close to the pressure. By Rayleigh's criterion conditions are optimum for a large input of energy to the instability.

(ii) Both forms of behaviour may exist in the duct, although convecting behaviour always exists for some distance downstream of the flame holder. The data imply that the transition from convecting to concurrent behaviour takes place at the axial position where the time-averaged conical flame has spread radially from the gutter lip to impinge on the walls of the duct. At this position the mean flame area, and hence the mean C_2 emission per unit length, is maximum. We suggest this is the limit of influence of the flame holder and that beyond it the flame no longer exists as a connected sheet. In this region the combustion is taking place in the pockets formed by the large coherent eddies.

(iii) When convecting behaviour exists along most of the duct, oscillations of small but measurable magnitude occur. We term the instability weak buzz. Established buzz occurs when concurrent behaviour occupies the most significant portion of the duct. This results in a large increase in the magnitude of the instability.

(iv) The transition from weak to established buzz occurs sharply and with little change in mean flow conditions. The transition is associated with an abrupt change in frequency as well as an increase in amplitude, and a change in the shape of the modal pressure and heat release rate distributions. Once the transition has taken place, the mode of coupling is tolerant to large changes in mean flow conditions which then vary the magnitude of modal distributions but maintain the shape.

(v) The peak in the mean C_2 emission is significantly closer to the gutter lip during established buzz than during weak buzz. This shape is approximately mimicked by the unsteady C_2 emission.

(vi) An adequate prediction of buzz frequency and pressure mode shape does not require a detailed description of the flame motion. But it must consider the resulting pattern of C_2 emission along the entire duct, since the region local to the gutter plays a minor role in the total contribution to the energy input to the flame. Further, the boundary conditions are vital in determining the total energy balance in the duct. It will be shown in Part 2 that the frequency, growth rate and modal distributions can be predicted within 7% by an acoustic model including the motion of a flame front and the distributed heat release downstream of it. However, the model is unable to predict the nonlinear part of the problem; that is whether weak or established buzz exists within the duct.

This work was gencrously funded by Rolls-Royce plc and was carried out at the Whittle Laboratory, Cambridge University Engineering Department. The author is particularly grateful to Mr A. Sotheran and Mr J. Lewis of Rolls-Royce for their interest and enthusiastic support. A very great contribution has also been made by the author's colleagues, Drs A. P. Dowling and G. J. Bloxsidge. Much of the design of the combustion apparatus is due to Mr P. Turner. The experimental project would not have been possible without the technical ingenuity and skill of Mr N. Hooper.

REFERENCES

Baade, P. K. 1978 Design criteria and models for preventing combustion oscillations. *Proc. ASHRAE Symp. on Combustion-Driven Oscillations, Atlanta.*

Bendat, J. S. & Piersol, A. G. 1971 *Random Data: Analysis and Measurement Procedures.* Wiley-Interscience.

Bloxsidge, G. J. 1987 Reheat buzz. An acoustically driven combustion instability. Ph.D. dissertation, University of Cambridge.

Bloxsidge, G. J., Dowling, A. P. & Langhorne, P. J. 1988 Reheat buzz: an acoustically coupled combustion instability. Part 2. Theory. *J. Fluid Mech.* **193**, 445–473.

Campbell, I. G., Bray, K. N. C. & Moss, J. B. 1983 Combustion oscillations in a ducted premixed flame. *I. Mech. E. Intl Conf. on Combustion in Engineering, Oxford*, pp. 85–94.

Clark, W. H. & Humphrey, J. W. 1986 Identification of longitudinal acoustic modes associated with pressure oscillations in ramjets. *J. Propulsion and Power* **2**, 199–205.

Dines, P. G. 1983 Active control of flame noise. Ph.D. dissertation, University of Cambridge.

Gaydon, A. G. 1974 *The Spectroscopy of Flames.* Chapman & Hall.

Hedge, U. G., Reuter, D., Zinn, B. T. & Daniel, B. R. 1987 Fluid mechanically coupled combustion instabilities in ramjet combustors. *AIAA*-87-0216.

Heitor, M. V., Taylor, A. M. K. P. & Whitelaw, J. H. 1984 Influence of confinement on combustion instabilities of premixed flames stabilized on axisymmetric baffles. *Combust. Flame* **57**, 109–121.

Hurle, I. R., Price, R. B., Sugden, T. M. & Thomas, A. 1968 Sound emission from open turbulent premixed flames. *Proc. R. Soc. Lond.* A **303**, 409–427.

Katsuki, M. & Whitelaw, J. H. 1986 The influence of duct geometry on unsteady premixed flames. *Combust. Flame* **63**, 87–94.

Keller, J. O., Vaneveld, L., Korschelt, D., Hubbard, G. L., Ghoniem, A. F., Daily, J. W. & Oppenheim, A. K. 1981 Mechanism of instabilities in turbulent combustion leading to flashback. *AIAA J.* **20**, 254–262.

Lewis, J. S. 1967 The effect of local fuel concentration on reheat jet pipe vibrations. *Intl Symp. on Combustion in Advanced Gas Turbine Systems, Cranfield.*

Mugridge, B. D. 1980 Combustion driven oscillations. *J. Sound Vib.* **70**, 437–452.

Poinsot, T., Trouve, A. C., Veynante, D. P., Candel, S. M. & Esposito, E. 1987 Vortex driven acoustically coupled combustion instabilities. *J. Fluid Mech.* **177**, 265–293.

Price, R. B., Hurle, I. R. & Sugden, T. M. 1968 Optical studies of the generation of noise in turbulent flames. *12th Symp. (Intl) on Combustion*, pp. 1093–1102.

Putnam, A. A. 1971 *Combustion-Driven Oscillations in Industry.* Elsevier.

Putnam, A. A. & Faulkner, L. 1982 An overview of combustion noise. *J. Energy* **7**, 458–469.

Ramachandra, M. K. & Strahle, W. C. 1983 Acoustic signature from flames as a combustion diagnostic tool. *AIAA J.* **21**, 1107–1114.

Rayleigh, J. W. S. 1896 *The Theory of Sound.* Macmillan.

Reuter, D., Daniel, B. R., Jagoda, J. & Zinn, B. T. 1986 Periodic mixing and combustion processes in gas fired pulsating combustors. *Combust. Flame* **65**, 281–290.

Sankar, S. V., Jagoda, J. I., Daniel, B. R. & Zinn, B. T. 1987 Flame driving of axial acoustic waves: comparison of theoretical predictions and experimental observations. *AIAA*-87-0219.

Schadow, K. C., Gutmark, E., Parr, T. P., Parr, D. M. & Wilson, K. J. 1987 Enhancement of fine-scale mixing for fuel-rich plume combustion. *AIAA*-87-0376.

Schöyer, H. F. R. 1983 Incomplete combustion: a possible cause of combustion instability. *AIAA J.* **21**, 1119–1126.

Shivashankara, B. N., Strahle, W. C. & Handley, J. C. 1975 Evaluation of combustion noise scaling laws by an optical technique. *AIAA J.* **13**, 623–627.

Sivasegaram, S. & Whitelaw, J. H. 1987 Oscillations in confined disk-stabilised flames. *Combust. Flame* **68**, 121–130.

Smart, A. E., Jones, B. & Jewell, N. T. 1976 Measurements of unsteady parameters in a rig designed to study reheat combustion instabilities. *AIAA*-76-141.

Smith, D. A. & Zukoski, E. E. 1985 Combustion instability sustained by unsteady vortex combustion. *AIAA*-85-1248.

Snellink, G. 1973 Optical measurements on premixed flames to locate the noise sources. *Combustion Institute European Symp., Sheffield*, pp. 553–558.

STERLING, J. D. & ZUKOSKI, E. E. 1987 Longitudinal mode combustion instabilities in a dump combustor. *AIAA*-87-0220.

TIDGEMAN, H. 1975 On the propagation of sound waves in cylindrical tubes. *J. Sound Vib.* **39**, 1–33.

VANEVELD, L., HOM, K. & OPPENHEIM, A. K. 1984 Secondary effects in combustion instabilities leading to flashback. *AIAA J.* **22**, 81–82.

YAMAGUCHI, S., OHIWA, N. & HASEGAWA, T. 1985 Structure and blow-off mechanisms of rod-stabilised premixed flame. *Combust. Flame* **62**, 31–41.

YOSHIDA, A. & TSUJI, H. 1984 Mechanism of flame wrinkling in turbulent premixed flames. *12th Symp. (Intl) on Combustion*, pp. 445–451.

ZUKOSKI, E. E. 1978 *Afterburners.* In *The Aerothermodynamics of Gas Turbine Engines* (ed. G. C. OATES), *Rep. No. AFAPL-TR*-78-52.